

Improved color rendering and luminous efficacy in phosphor-converted white light-emitting diodes by use of dual-blue emitting active regions

Roya Mirhosseini¹, Martin F. Schubert¹, Sameer Chhajed¹, Jaehee Cho¹, Jong Kyu Kim¹, and E. Fred Schubert^{1,2,*}

Future Chips Constellation, Rensselaer Polytechnic Institute, Troy, NY 12180 USA

¹*Department of Electrical, Computer, and Systems Engineering, Rensselaer Polytechnic Institute, Troy, NY 12180 USA*

²*Department of Physics, Applied Physics, and Astronomy, Rensselaer Polytechnic Institute, Troy, NY 12180 USA*
**efschubert@rpi.edu*

Abstract: Conventional white-light sources suffer from a fundamental trade-off between color rendering index and the luminous efficacy; increasing one generally comes at the expense of the other. We demonstrate through simulation that dual-wavelength blue-emitting active regions in phosphor-converted white light sources maximize the output luminous flux while significantly increasing the color rendering ability. Our results indicate that such improvements can be achieved over a broad range of correlated color temperatures.

©2009 Optical Society of America

OCIS codes: 230.3670 (Light-emitting diodes); 330.1715 (Color, rendering and metamerism)

References and links

1. E. F. Schubert, and J. K. Kim, "Solid-state light sources getting smart," *Science* **308**(5726), 1274–1278 (2005).
2. A. Zukauskas, R. Vaicekauskas, F. Ivanauskas, R. Gaska, and M. S. Shur, "Optimization of white polychromatic semiconductor lamps," *Appl. Phys. Lett.* **80**(2), 234–237 (2002).
3. J. Tsao, "Solid-state lighting: lamps, chips and materials for tomorrow," *IEEE Circuits Devices Mag.* **20**(3), 28–37 (2004).
4. S. W. Brown, C. Santana, and G. P. Eppeldauer, "Development of a tunable LED-based colorimetric source," *J. Res. Natl. Inst. Stand. Technol.* **107**, 363–371 (2002).
5. B. Damilano, N. Grandjean, C. Pernot, and J. Massies, "Monolithic white light emitting diodes based on InGaN/GaN multiple quantum wells," *Jpn. J. Appl. Phys.* **40**(Part 2, No. 9A/B), 918–920 (2001).
6. S. Chhajed, Y. Xi, Y. L. Li, T. Gessmann, and E. F. Schubert, "Influence of junction temperature on chromaticity and color-rendering properties of trichromatic white-light sources based on light-emitting diodes," *J. Appl. Phys.* **97**(5), 054506 (2005).
7. E. F. Schubert, *Light Emitting Diodes* (Cambridge University Press, Cambridge, U.K. 2003), Chap. 19–20.
8. R. J. Xie, and N. Hirotsuki, "Review: Silicon-based oxynitrides and nitride phosphors for white LEDs," *Sci. Technol. Adv. Mater.* **8**(7-8), 588–600 (2007).
9. T. Mukai, *Proceedings of SPIE Photonics West, San Jose, California, Jan. 29, 7216* (2009)
10. R. Mueller-Mach, G. Mueller, M. R. Krames, H. A. Hoppe, F. Stadler, W. Schnick, T. Juestel, and P. Schmidt, "Highly efficient all-nitride phosphor-converted white light emitting diode," *Phys. Status Solidi A* **202**(9), 1727–1732 (2005).
11. S. Nakamura, "Progress with GaN-based blue/green LEDs and bluish-purple semiconductor LEDs," *Electron. Commun. Jpn.* **81**, 1–8 (1998).
12. M. Peter, A. Laubsch, P. Stauss, A. Walter, J. Baur, and B. Hahn, "Green ThinGaN power LED-demonstrates 100 lm," *Phys. Status Solidi C* **5**(6), 2050–2052 (2008).
13. M. Yamada, Y. Narukawa, and T. Mukai, "Phosphor free high-luminous-efficiency white light-emitting diodes composed of InGaN multi-quantum well," *Jpn. J. Appl. Phys.* **41**(Part 2, No. 3A), 246–248 (2002).
14. I. K. Park, J. Y. Kim, M. K. Kwon, C. Y. Cho, J. H. Lim, and S. J. Park, "Phosphor-free white light emitting diode with laterally distributed multiple quantum wells," *Appl. Phys. Lett.* **92**(9), 091110 (2008).
15. M. Grundmann, and U. Mishra, "Multi-color light emitting diode using polarization-induced tunnel junctions," *Phys. Status Solidi C* **4**(7), 2830–2833 (2007).
16. International Commission on Illumination, *Method of measuring and specifying colour rendering properties of light sources*, ISBN 978–3900734572 (1995)

1. Introduction

Semiconductor white light-emitting diodes (LEDs) have attracted a great deal of attention in solid-state lighting applications. Due to their potential for substantial energy savings, high efficiency, small size, and long lifetime, it has been projected that LEDs will broadly replace conventional incandescent and fluorescent lamps for general lighting in the future [1–4]. To create white light from LEDs, two distinct approaches have been adopted: (i) use of individual primary-color LEDs (such as red, green, and blue, also known as RGB), and (ii) the combination of wavelength down-converting phosphor with a blue or ultraviolet LED [5]. The multichip RGB approach allows for high color rendition, chromaticity-point stabilization, and color adjustment [2,6]. However, strong temperature dependence of performance and high cost are among the main disadvantages. Phosphor-converted white LEDs benefit from relatively low cost as well as great color stability over a wide range of temperatures [7]. White LEDs based on cerium-doped yttrium aluminum garnet (YAG:Ce) yellow phosphor have been used in various markets. Recent publications on a new class of inorganic phosphors, oxynitride and nitride luminescent materials, report promising results and encourage the use of these phosphors in solid-state lighting applications [8].

Two of the key quantities in light source assessment are luminous efficacy of radiation (LER), and color rendering index (CRI). LER, given by Eq. (1), measures the optical efficiency of the light emitted by a source, and is determined solely by the spectrum (resistive electrical losses do not affect the LER).

$$LER = 683 \frac{\text{lm}}{\text{W}} \frac{\int_{\lambda} P_{\text{white}}(\lambda) V(\lambda) d\lambda}{\int_{\lambda} P_{\text{white}}(\lambda) d\lambda}, \quad (1)$$

where the pre-factor 683 lm/W is a normalization factor, $P_{\text{white}}(\lambda)$ is the spectral power density (SPD) of the white light source and $V(\lambda)$ is the eye sensitivity function, with 555 nm being the most sensitive wavelength to the human eye [7]. Another figure of merit for light sources is luminous efficacy of the source (LES), which is defined as the ratio of luminous flux to input electrical power. A record high LES for GaInN white LEDs has been reported by Mukai, 249 lm/W at 20 mA and 145 lm/W at 350 mA [9], corresponding to equivalent of two- to three-fold improvements over standard fluorescent sources and an order of magnitude enhancement over standard incandescent sources.

The CRI is another critical characteristic of light sources for general lighting applications. The color rendering performance of a source is determined by its spectral power distribution. High CRIs generally require a broad emission spectrum distributed throughout the visible region; the sun and blackbody radiation have a CRI of 100. Generally for illumination purposes, CRI values in the 70s are considered 'acceptable', and values greater than 80 are regarded as 'good' [10].

While high color rendering ability is best attained by broad spectral distribution of the emission band throughout the visible region, the LER of a source is highest for monochromatic light sources radiating at 555 nm. A function that optimizes the trade-off between CRI and LER in multichip solid-state lamps is given by:

$$F_{\sigma}(\lambda_1, \dots, \lambda_n, \Delta\lambda_1, \dots, \Delta\lambda_n, I_1, \dots, I_n) = \sigma LER + (1 - \sigma) CRI, \quad (2)$$

where σ is a weighting factor that regulates the trade-off between the efficacy and color rendition ($0 \leq \sigma \leq 1$), n is the number of primary LEDs and λ_i , $\Delta\lambda_i$, and I_i are peak wavelengths, spectral linewidths, and the luminous fluxes of the primary sources, respectively. Although dichromatic white-light sources offer the highest LER, they suffer

from a low CRI. Studies have shown that trichromatic and tetrachromatic white-light LED lamps achieve a great balance between CRI and LER [2,6]. However, a key element associated with the future penetration of LEDs into the solid-state lighting market is LER, and this parameter is reduced with increasing LED quantity.

In this investigation, we analyze single-chip phosphor-converted white-light sources with single-wavelength blue-emitting active regions and dual-wavelength blue-emitting active regions. We demonstrate through simulation that dual-blue white sources are more efficient devices, enhancing both CRI and LER, compared to single-blue white sources. Dual-blue emission takes advantage of the exponential dependence of the eye sensitivity function on wavelength in the blue spectral region by allowing one of its two emission peaks to lie closer to the peak eye sensitivity wavelength than the single-blue emission, thereby increasing the LER. We also show that dual-blue emitting active regions broaden the emission spectrum, and result in higher CRI values.

2. LED-based white light source comprised of dual-color emitting active regions

Dual-color LEDs with two distinct energy-gaps in the blue and green spectral regions have been a topic of active research [11–15]. A significant challenge in these devices is the loss of light due to photon absorption in the lower energy-gap quantum well. Blue GaInN quantum wells (QWs) require 10-15% In content, while green QWs demand 15-20%. An increase in the In composition, results in lattice mismatch between GaInN and GaN which brings about strain between the GaN barrier layer and the GaInN well layer [11]. However, reabsorption is less significant in dual-blue LEDs compared to dual-color LEDs (e.g. blue and green), because of the proximity of the two emission wavelengths.

Recent experimental results indicate much improvement in LEDs with dual-color emitting active regions. Peter et al. reported an efficient multi-quantum well (MQW) structure with six blue and one green QW showing 123 lm/W at 100 mA and 80 lm/W at 350 mA [12]. Yamada et al. successfully demonstrated growth and fabrication of phosphor-free white LED emitting with dual-wavelength emitting active regions (blue and yellow wavelengths) and multi-color active regions (blue, green and red wavelengths) [13]. Park et al. reported a laterally stacked structure of blue and green GaInN-based MQWs with two distinct photoluminescence emission peaks [14]. Finally, Grundmann et al. reported a multi-color LED, with stacked active regions emitting at 405 nm and 490 nm, containing a polarization induced tunnel junction [15].

3. Phosphor-converted white light source consisting of dual-blue emitting MQWs

In our simulation we use the absorption and emission spectra of commercial YAG:Ce yellow phosphor with peak emission wavelength of 577 nm, illustrated in Fig. 1(a). Two different sets of LED structures, single-blue and dual-blue emitting active regions, with peak emission wavelengths in the 430-500 nm range are considered. The SPD function of an LED can be described by a Gaussian function; therefore,

$$P(\lambda) = \frac{1}{\sigma\sqrt{2\pi}} \exp\left[-\frac{1}{2}\left(\frac{\lambda - \lambda_{peak}}{\sigma}\right)^2\right], \quad (3)$$

where P is the optical power, ΔE is the full-width at half-maximum linewidth of the LED emission, and σ is defined as:

$$\sigma = \frac{\lambda_{peak}^2 \Delta E}{2hc\sqrt{2\ln 2}}. \quad (4)$$

We use spectral linewidth of $\Delta E = 5k_B T$, which is comparable to the linewidth of blue GaInN emitters, but narrower than the GaInN green emitters and broader than the AlGaInP

red emitters [7]. Based on the overlap of phosphor absorption spectrum and the blue LED spectrum, the number of photons absorbed by the phosphor per second is calculated as follows:

$$photon_{abs} = \int \frac{P_{blue}(\lambda)}{hc/\lambda} [1 - \exp(-P_{abs}(\lambda)t)] d\lambda, \quad (5)$$

where t denotes the phosphor thickness, and $P_{abs}(\lambda)$ is the phosphor absorption spectrum. Conversion of pumped LED power into yellow power is given as:

$$P_{yellow}(\lambda) = photon_{abs} \eta P_{ems}(\lambda), \quad (6)$$

where η is the quantum efficiency of the phosphor and $P_{ems}(\lambda)$ is the phosphor emission spectrum. The SPD of phosphor-converted white light source is given as:

$$P_{white}(\lambda) = P_{emtBlue}(\lambda) + P_{yellow}(\lambda), \quad (7)$$

where, $P_{emtBlue}(\lambda)$ is the blue power transmitted through the phosphor. Using the Newton-Raphson method, the required phosphor thickness is calculated at correlated color temperatures (CCTs) ranging from 3500 K to 8500 K. The calculated phosphor thicknesses for single-blue and dual-blue emitting active regions at a given CCT are similar, and therefore, the corresponding scattering losses will also be comparable. The general CRI is then calculated by taking into account the adaptive color shift. Figure 1(a) illustrates the absorption and emission spectra of YAG:Ce, and Fig. 1(b) shows the spectral power density of (solid) dual-blue white source with emission peaks at 435 nm and 489 nm and a CCT of 5600 K and (dashed) single-blue white source with peak wavelength of 471 nm at 4100 K. The two white-light sources' spectra in Fig. 1(b) correspond to the highest attainable values of the CRI.

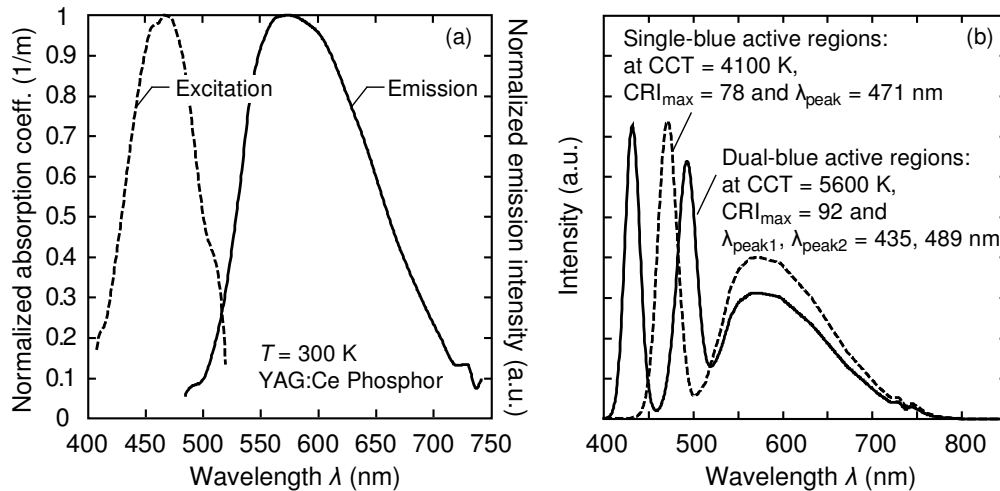


Fig. 1. Phosphor and white light spectra: (a) (dashed) excitation and (solid) emission spectra of YAG:Ce phosphor, and (b) emission spectra of phosphor-converted white-light sources with (dashed) single-blue white source and (solid) dual-blue white source.

Figure 2 depicts the chromaticity diagram in the (u, v) coordinate system; indicated in Fig. 2 are locations of the YAG:Ce phosphor, blue LED peak emission wavelengths, and the single- and dual-blue white light sources, each of which corresponds to the maximum achievable CRI of 78 and 92 at 4100 K and 5600 K (spectra of both white sources are shown in Fig. 1(b)).

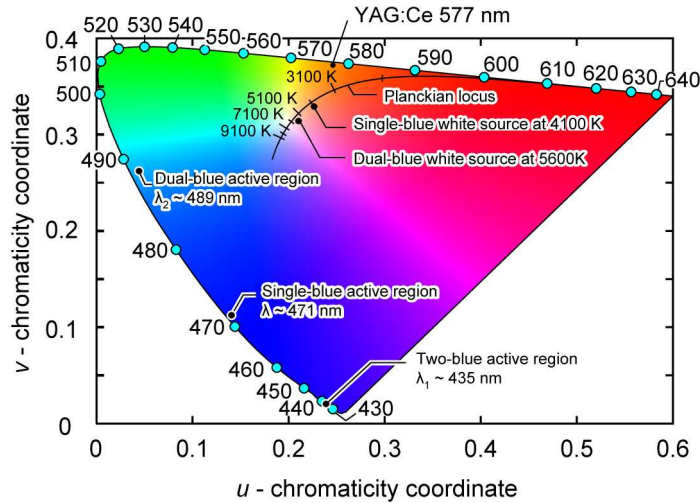


Fig. 2. The chromaticity diagram based on CIE 1964 (u,v) color space. Included are the YAG:Ce phosphor, blue LED peak wavelengths, and single-blue and dual-blue white sources. The two white sources exhibit the highest achievable CRIs.

Figure 3 shows the CRI and LER contour plots as functions of the two emission-peak wavelengths, λ_1 and λ_2 for a CCT of 5600 K. It is well known that sources at distances greater than 0.0054 ($d = \sqrt{\Delta u^2 + \Delta v^2}$) from the Planckian locus are not true white light sources [16]. However, in order to observe the difference between the single-blue and dual-blue white sources, Fig. 3 includes all simulated white light sources regardless of their distance from the Planckian locus. In both contour plots, single-blue wavelengths are represented by points lying diagonally across from bottom left corner to top right corner, and dual-blue wavelengths are off the diagonal. CRI of single-blue white sources have peak CRI values in the high 70s, whereas dual-blue white sources offer CRIs in low-90s. In addition, impact of eye sensitivity function manifests itself in Fig. 3(b); LER gradually increases as peak wavelengths approach 500 nm.

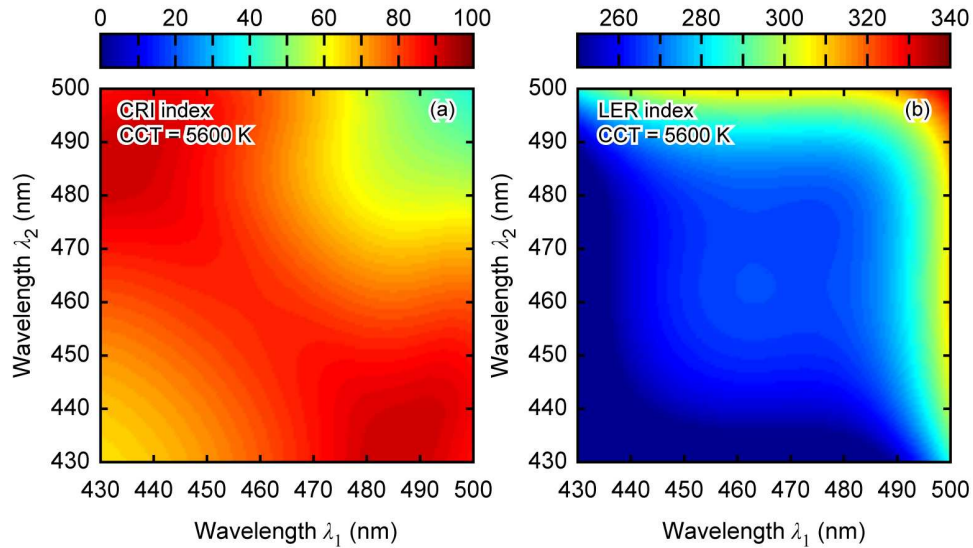
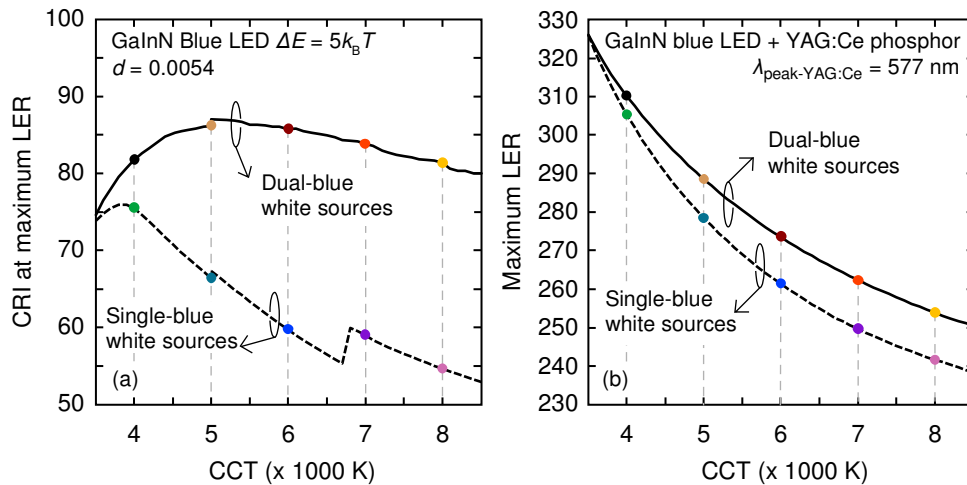


Fig. 3. Simulated white light sources as functions of blue emission peaks: λ_1 and λ_2 at 5600 K. (a) Color Rendering Index (CRI), and (b) luminous efficacy of radiation (LER).

In the following figures only white sources within a distance of 0.0054 from the Planckian locus are considered. Figure 4 displays the CRI and LER as functions of CCT for both single-blue and dual-blue white sources. The small discontinuity at 5000 K in Fig. 4(a) is a well-known artifact resulting from the use of different reference sources in calculating the CRI [17]; black-body radiation is used as reference source below 5000 K and CIE standard illuminant D is used at higher temperatures [17]. The CRI values in Fig. 4(a) correspond to blue-wavelengths that are chosen to produce maximum achievable LER values for both types of white sources. Single-blue white sources experience a 30% drop in their CRIs derived at maximum LERs, decreasing from 76 at 3800 K to 53 at 8500 K. In contrast, dual-blue white sources, with peak of 87 at 5100 K, experience a minor reduction in CRI. The discontinuity in CRI of single-blue white sources at 6700 K is due to the decrease in blue peak wavelengths at higher CCTs; the phosphor coordinate and the arch in the Planckian locus force LEDs towards shorter wavelengths. At this discontinuity, the maximum achievable LER location changes from the top end of the $d = 0.0054$ limitation (above the Planckian locus) to the lower end of the $d = 0.0054$ limitation (below the Planckian locus). LER values for sources that lie at distances greater than $d = 0.0054$ from the Planckian locus, which are not “true white” sources and they are not shown in Fig. 4, range from 375 lm/W at 3500 K to 290 lm/W at 8500 K. The blue peak-wavelengths corresponding to the maximum LER values are listed in the table below Fig. 4.

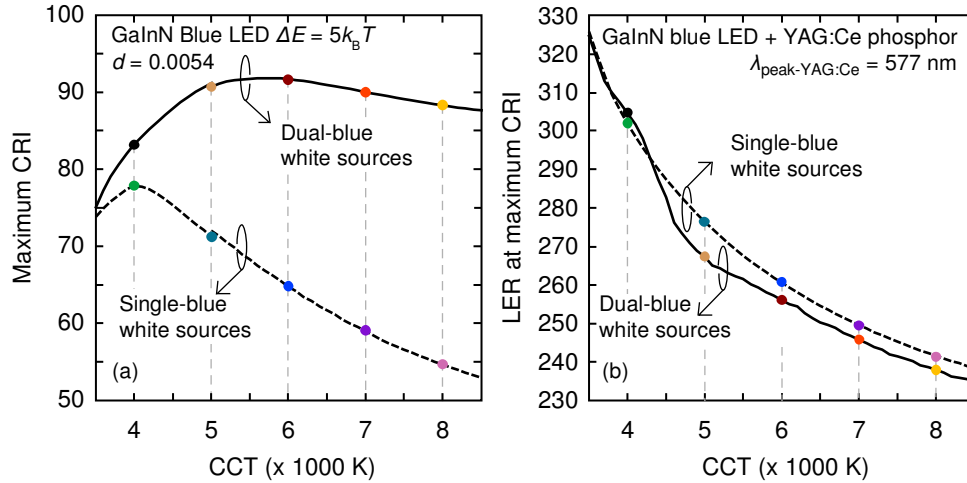


CRI is obtained at maximum LER at the following blue emission wavelengths, λ_{peak} (nm):					
CCT (K)	4000	5000	6000	7000	8000
Dual-blue $\lambda_{\text{peak1}}, \lambda_{\text{peak2}}$ (nm)	● 452, 489	● 450, 491	● 451, 492	● 450, 492	● 450, 492
Single-blue λ_{peak} (nm)	● 475	● 478	● 479	● 475	● 476

Fig. 4. CRI and LER dependence on CCT, shown from 3500 K to 8500 K (dashed) single-blue white sources, and (solid) dual-blue white sources: (a) CRIs corresponding to blue peak wavelengths that produce maximum LER, and (b) maximum achievable LER in white sources that lie within distance of 0.0054 from the Planckian locus. The blue emission wavelengths, λ_{peaks} , specified in the table produce the maximum achievable LERs; λ_{peaks} are known values that are used as inputs to Eq. (3).

Figure 5(a) shows the maximum achievable CRI for the two structures; Fig. 5 differs from Fig. 4 which displays points corresponding to maximum calculated LER. Similar to Fig. 4, single-blue white sources drop in CRI by $\sim 32\%$, decreasing from 78 at 3500 K to 53 at 8500 K. The dual-blue white sources peaks remain stable in the high 80s and low 90s from 5000 K to 8500 K. In Fig. 5(b), we observe that LER at maximum CRI for dual-blue is slightly lower

than single-blue white source. The table below the Fig. 5 lists the CCT and the peak wavelengths, λ_{peak} , corresponding to maximum CRIs for both single-blue and dual-blue white sources.



Maximum CRI is obtained at the following blue emission wavelengths, λ_{peak} :					
CCT (K)	4000	5000	6000	7000	8000
Dual-blue $\lambda_{\text{peak1}}, \lambda_{\text{peak2}}$ (nm)	● 439, 489	● 433, 489	● 436, 490	● 436, 490	● 436, 490
Single-blue λ_{peak} (nm)	● 470	● 474	● 475	● 475	● 476

Fig. 5. CRI and LER dependence on CCT, shown from 3500 K to 8500 K (dashed) single-blue white sources, and (solid) dual-blue white sources: (a) maximum achievable CRI s, and (b) LER values corresponding to wavelengths that produce the maximum CRI. Only sources within a distance of 0.0054 from the Planckian locus are considered. The blue emission wavelengths, λ_{peaks} , specified in the table produce the maximum achievable CRIs; λ_{peaks} are known values that are used as inputs to Eq. (3).

Dual-blue white sources benefit from higher values of the CRI due to broader white light spectra. Figure 6 illustrates the special CRIs, CRI_i , for the eight CIE test-color samples. Each bar represents an average CRI_i value of either the single-blue- or dual-blue-white light source with CCTs ranging from 3500 K to 8500 K. We observe that dual-blue white sources display a significant gain over single-blue white sources across the entire CCT array. Particularly significant enhancements are evident in CRI_3 , CRI_4 , CRI_7 , and CRI_8 , corresponding to strong yellow green, moderate yellowish green, light violet, and light reddish purple test-color samples, respectively.

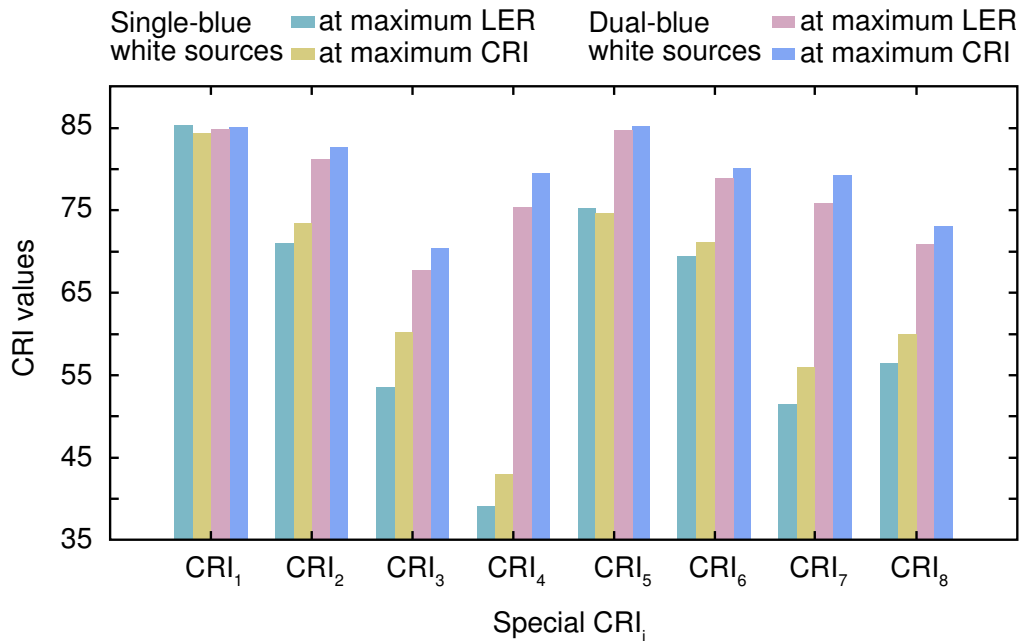


Fig. 6. Special CRI values of the set of eight test-color samples for the single-blue- and dual-blue white sources at maximum achievable LERs and CRIs.

4. Conclusion

We have analyzed phosphor-converted white-light sources with GaInN blue LEDs for both single-blue and dual-blue emitting active regions. We show significant enhancements in color rendition ability and luminous efficacy across the entire range of CCTs. Dual-blue white sources can be tuned to achieve higher CRIs and LERs, as opposed to single-blue white sources. The notable improvements in the two key lighting parameters establish the dual-blue emitting active region as an efficient and high quality approach to white light generation.

Acknowledgments

The authors gratefully acknowledge support by the National Science Foundation, the Department of Energy, Sandia National Laboratories, New York State, Samsung Electro-Mechanics Company, Crystal IS Corporation, and Troy Research Corporation.